Original Research *Featured Article*

Inhibition of glutathione synthesis distinctly alters mitochondrial and cytosolic redox poise

Vladimir L Kolossov[1], William P Hanafin[1], Jessica N Beaudoin[1,2], Denisa E Bica[1], Stephen J DiLiberto[1,2], Paul JA Kenis[1,3] and H Rex Gaskins[1,2,4,5]

[1]Institute for Genomic Biology, University of Illinois at Urbana-Champaign, Urbana, IL 61801, USA; [2]Departments of Animal Sciences, University of Illinois at Urbana-Champaign, Urbana, IL 61801, USA; [3]Chemical & Biomolecular Engineering, University of Illinois at Urbana-Champaign, Urbana, IL 61801, USA; [4]Pathobiology, University of Illinois at Urbana-Champaign, Urbana, IL 61801, USA; [5]Division of Nutritional Sciences, University of Illinois at Urbana-Champaign, Urbana, IL 61801, USA
Corresponding author: Vladimir L Kolossov. Email: viadimer@illinois.edu

Abstract

The glutathione couple GSH/GSSG is the most abundant cellular redox buffer and is not at equilibrium among intracellular compartments. Perturbation of glutathione poise has been associated with tumorigenesis; however, due to analytical limitations, the underlying mechanisms behind this relationship are poorly understood. In this regard, we have implemented a ratiometric, genetically encoded redox-sensitive green fluorescent protein fused to human glutaredoxin (Grx1-roGFP2) to monitor real-time glutathione redox potentials in the cytosol and mitochondrial matrix of tumorigenic and non-tumorigenic cells. First, we demonstrated that recovery time in both compartments depended upon the length of exposure to oxidative challenge with diamide, a thiol-oxidizing agent. We then monitored changes in glutathione poise in cytosolic and mitochondrial matrices following inhibition of glutathione (GSH) synthesis with L-buthionine sulphoximine (BSO). The mitochondrial matrix showed higher oxidation in the BSO-treated cells indicating distinct compartmental alterations in redox poise. Finally, the contributory role of the p53 protein in supporting cytosolic redox poise was demonstrated. Inactivation of the p53 pathway by expression of a dominant-negative p53 protein sensitized the cytosol to oxidation in BSO-treated tumor cells. As a result, both compartments of PF161-T+p53^{DD} cells were equally oxidized $\approx$20 mV by inhibition of GSH synthesis. Conversely, mitochondrial oxidation was independent of p53 status in GSH-deficient tumor cells. Taken together, these findings indicate different redox requirements for the glutathione thiol/disulfide redox couple within the cytosol and mitochondria of resting cells and reveal distinct regulation of their redox poise in response to inhibition of glutathione biosynthesis.

Keywords: Live cell imaging, cytosol, mitochondria, redox probe, glutathione, p53

***Experimental Biology and Medicine* 2014; 239: 394–403. DOI: 10.1177/1535370214522179**

Introduction

The intracellular redox environment is crucial in integrating multiple metabolic, signaling, and transcriptional processes.[1–3] GSH, the most prominent redox buffer, is synthesized in the cytoplasm and distributed to at least nine different subcellular compartments.[1,4,5] GSH protects cells against oxidative stress through two electron reduction of oxidants with concomitant oxidation of GSH to GSSG. GSH protects against reactive oxygen species (ROS) by serving as a co-factor for several detoxifying enzymes, including glutathione peroxidase, glutathione transferase, and glutaredoxin.[6,7] In addition, GSH reacts spontaneously with intracellular ROS producing GSSG. GSSG is then effectively reduced back to GSH by glutathione reductase (GR), which requires NADPH as an electron donor.[8] The redox chemistry of the glutathione pool is characterized by the glutathione redox potential (E_{GSH}), which depends on the GSH/GSSG ratio as well as total glutathione content.

Multiple studies have demonstrated that E_{GSH} is compartmentalized and not at redox equilibrium among organelles.[1,9–14] Moreover, accumulating evidence indicates that the glutathione poise of subcellular compartments dynamically and independently alters cellular responsiveness to physiological stimuli.[15–18] Measurements of compartmentalized E_{GSH} is a significant methodological challenge, as early methods quantified GSH/GSSG ratios at cellular or organellar levels after cell disruption and are limited in spatiotemporal resolution of intraorganellar E_{GSH} change. Recently, several variants of redox-sensitive green

fluorescent protein (roGFP) probes have been developed with a suitable range of redox potentials[19–21] to measure compartment-specific glutathione redox potentials including those within the cytosol and mitochondria in living cells.[4,17,18,22–25] Most recently, human glutaredoxin 1 (Grx1) was fused to the roGFP2 probe to improve specificity and speed of thiol-disulfide exchange with intracellular GSH/GSSG couple.[21,26] The probe is considered to be a pH-independent indicator for changes of E_{GSH} in the pH range between 5.5 and 8.0.[21,26]

The maintenance of optimal E_{GSH} among subcellular compartments is critical to cell survival, integrating multiple metabolic, signaling and transcriptional processes; therefore, tight regulation of glutathione homeostasis is necessary. Although most GSH is localized in the cytosol, a distinctly regulated pool is present in the mitochondrial matrix accounting for 10–15% of total cellular GSH.[12] Among the antioxidants and detoxifying enzymes existing in mitochondria, GSH acts to repair or avoid oxidative modifications that lead to mitochondrial dysfunction and cell death and thereby serves as the main defense for maintenance of redox homeostasis in this organelle.[5,7,12,27] Antioxidant capacity of mitochondria is especially important considering that mitochondria are the primary intracellular site of oxygen consumption and the major source of ROS. Mitochondrial ROS have been proven biologically important in a variety of physiological processes, including adaptation to hypoxia, regulation of autophagy, regulation of immunity, differentiation, and as a signaling intermediate to facilitate cellular adaptation to stress.[12,27–29] Real-time monitoring of dynamic changes of cytosolic and matrix E_{GSH} pools have revealed independent adaptation to environmental changes.[17,18,23,30]

Recent experimental evidence indicates that ROS are critically involved in tumor cell functions.[31,32] Additionally, it is now clear that tumor suppressor p53, a transcription factor, is a major regulator of cellular redox state.[33–35] For instance, activation by p53 of a mitochondrial glutaminase facilitates hydrolysis of glutamine to glutamate, which in turn can be used to generate GSH leading to an increased GSH/GSSG ratio.[36] Mutations of the p53 gene and consequent post-translational alterations of the p53 protein are frequently observed in a wide variety of human cancers known to have a poor outcome.[37] The relationship between p53 and the cellular redox system is bidirectional, as p53 activity is regulated by redox-dependent signals, and in turn, modulates the intracellular redox balance.[33,35]

The aim of this study was to examine the contribution of *de novo* GSH synthesis to the maintenance of glutathione poise in the cytosol and mitochondrial matrix in tumorigenic and non-tumorigenic cells. Next, we examined the distinct effect of altered p53 activity on compartmental redox status in GSH deficient tumorigenic fibroblast cells.

Materials and methods

Materials

Unless stated otherwise, reagents were obtained from Sigma (St. Louis, MO, USA). Lipofectamine 2000 and enzymes used for modifying DNA were purchased from Invitrogen (Carlsbad, CA, USA). The primers for cloning were ordered from IDT (Coralville, IA, USA). Plasmids pECFP-C1 and pIRESpuro3 were purchased from Clontech (Mountain View, CA, USA).

Cell culture, transfection, and cell sorting

Chinese hamster ovary (CHO), mouse glioma (GL261), and human embryonic kidney (HEK293) cells were grown at 37°C with 5% CO_2 in Dulbecco's Modified Eagle (DMEM) and PF161 cells in DMEM/F10 (Cell Media Facility, University of Illinois, Urbana, IL, USA). Culturing, transfection, and cell sorting were performed as previously described.[38,39] CHO, HEK293, and GL261 cells were obtained from ATCC (Manassas, VA, USA).

The porcine control (PF161-C) and isogenic tumor PF161-T−$p53^{DD}$ and PF161-T+$p53^{DD}$ fibroblasts were a gift from Dr. Lawrence Schook (University of Illinois, Urbana, IL, USA).

Genetic constructs

The Grx1-roGFP2 sensor was cloned into pIRES-puro3 from original pQE-60. Briefly, the PCR product of the Grx1-roGFP2 sensor obtained with the primers Cyto-For 5′-GCTAGCCATGGCTCAAGAGTTTGTGAACTGCAA-3′ and Cyto-Rev 5′-GGATCCTTACTTGTACAGCTCGT CCATGCCGAGAGT-3′ was ligated into NheI/BamHI sites of pIRES-puro3. The Mito-Grx1-roGFP2 probe originally cloned into retroviral pLPCX vector has the signal sequence from fungus *Neurospora crassa* adenosine triphosphate synthase protein 9 targeting mitochondrial matrix.[21] The probe was transferred from retroviral to mammalian plasmid vectors in three steps. First, the PCR product comprised mitochondrial signal sequence was obtained with the oligonucleotide primer set MTS-For 5′- CTGGTA CCGCTAGCATGGCCTCCACTCGTGTCCTCGCCT-3′ and MTS-Rev 5′- TTGGATCCATGGAAGAGTAGGCGCG CTTCTGGAAA-3′ and cloned into KpnI/BamHI sites of pUC19 (pUC19-Mito). Next, the Grx1-roGFP2 probe was cloned into NcoI/BamHI sites of pUC19-Mito (pUC19-Mito-Grx1-roGFP2). Finally, an NheI/BamHI DNA fragment of pUC19-mito-Grx1-roGFP2, which is mito-Grx1-roGFP2 was cloned into the same restriction sites of pECFP-C1 or pIRESpuro3. All PCR products were initially ligated into pCR2.1 (TOPO Kit, Invitrogen, USA) and sequenced. RoGFP2 in pEGFP-N1 and Grx1-roGFP2 in pQE60 and mito-Grx1-roGFP2 in pLPCX were kind gifts from Dr. James Remington (University of Oregon, OR, USA) and Dr. Tobias Dick (Cancer Research Center, Heidelberg, Germany), respectively.

Fluorescence microscopy

Image acquisition of living cells stably transfected with roGFP2 or Grx1-roGFP2 constructs were performed in μ-Slide eight well or μ-Slide VI channel, ibiTreat microscopy chambers (Ibidi, Munich, Germany) and maintained for 48 h. The cells were washed twice with Dulbecco's phosphate-buffered saline supplemented with 5% FBS and

10 mmol/L glucose prior to imaging. Perfusion of cells cultured in channels was performed with a PHD Ultra syringe pump (Harvard Apparatus, Holliston, MA, USA) at 200 μL/min. Images were collected as described previously.[38]

To visualize spatiotemporal changes of glutathione poise, raw data were exported to Zen 2009 software (Carl Zeiss) and converted into 395 nm and 494 nm sets of 12-bit TIF images. Next, the pixels belonging only to the probe were selectively segmented.[40] The calculated threshold was scaled by a fixed number for all images and the function ''graythresh'' was implemented in a home-written script in MATLAB (Natick, MA, USA). The pixel-by-pixel 395/494 nm false-color ratio pictures were directly calculated by dividing 395 nm on 494 nm images.

To confirm mitochondrial localization of the mtGrx1-roGFP2 probe in stably transfected CHO cells, 3D images were acquired on a Zeiss ELYRA super-resolution microscope.

GSH measurement

To quantify GSH concentration in live cells, membrane-permeable monochlorobimane (mBCl) was utilized as described elsewhere.[39]

Determination of reduction potential and half time

The extent of reduced Grx1-roGFP2 was determined as previously described.[20,21] Briefly, the amount of roGFP2 in reduced form was calculated from the ratio of reduced to oxidized roGFP2 in accordance with the equation

$$\frac{R}{1-R} = \frac{F - F_{ox}}{F_{red} - F} \times \frac{I_{ox}}{I_{red}}$$

where F, F_{ox}, and F_{red} are the 395:494 nm excitation ratios at steady state, full oxidation, and full reduction, respectively. I_{ox} and I_{red} are the fluorescence intensities at 494 nm of the entirely oxidized and reduced samples. Determination of the fully oxidized and reduced states of roGFP2 was implemented by the addition of diamide and dithiothreitol (DTT), respectively, in designated concentrations.

The reduction potential ($E^{0'}$) for the chosen redox sensor is then calculated with the Nernst equation.[1] At 298 K the reduction potential of roGFP2 was determined by

$$E^{0'} = E^{0'}_{roGFP2} - 29.6\,mV \times \log\left(\frac{R}{1-R}\right)$$

where $E^{0'}_{roGFP2}$ is the consensus average value of the midpoint redox potential for roGFP2 of −280 mV.[19]

To determine half time of the sensor recovery (the time that takes for the fully oxidized sensor to reach the midpoint between its oxidized and steady state) we ran an analysis of variance to determine if the decay was exponential. Based on this analysis, we determined that we have an exponential decay with P values of 5×10^{-34} and 3×10^{-27} for cytosol and mitochondria, respectively. The half time was calculated based on an exponential decay according to the equation

$$T_{\frac{1}{2}} = \frac{\log 2 \times T_t}{\log\left(\frac{F_{ox}}{F_t}\right)}$$

where F_{ox} and F_t are the 395:494 nm excitation ratios of the sensor at fully oxidized and partially oxidized state at any time point t, respectively. T_t is the time at time point t.

Statistical analysis

All data are reported as mean ± standard deviation (SD). Two-way analysis of variance (ANOVA) was performed using XLStat program (v 2011.4.01; Addinsoft, NY, USA) to determine the effect of buthionine sulphoximine (BSO) treatments on R (fraction of the probe in the reduced form) and GSH content. Significant differences between treatment means were determined with the Tukey test for multiple pairwise comparisons. $P < 0.05$ was considered statistically significant.

Results

The redox probe indicates recovery of cytosolic and mitochondrial matrix glutathione poise from acute oxidative challenge

Recently, we demonstrated that the cytosol of mammalian cells is capable of restoring a highly reduced resting glutathione poise within minutes after an acute oxidative insult is removed.[41] Previously it has been demonstrated that, in *Arabidopsis* leaves recovery of the mitochondrial matrix does not occur in the time frame necessary for cytosolic redox recovery.[30] Therefore, to ascertain whether mammalian cells are similar to plants in their reversible pattern of E_{GSH} after wash-out of an acute oxidative insult, stably transfected CHO lines were derived with the Grx1-roGFP2 sensor targeted to the cytosol and mitochondrial matrix. Localization of the probe fused to a mitochondrial matrix targeting signal was demonstrated as described elsewhere.[21] Mitochondria in stably transfected cells exhibited the characteristic tubular shape (Figure S1), while in the cytosol, fluorescence of the probe was diffusely distributed (Figure 1b$_0$).

To assess the antioxidant capacity of cytosol and mitochondrial matrix, recovery of glutathione poise was monitored after brief cell perfusion with diamide-supplemented medium. Recent evidence indicates that exposure to diamide does not trigger compartmental pH change, confirming that the probe equilibrates with GSH/GSSG.[42] Representative fluorescence images of cytosolic and mitochondrial Grx1-roGFP2 with corresponding ratiometric analysis are shown in Figure 1. In time course experiments, the cytosolic and mitochondrial sensors were monitored initially at steady state for several minutes. The microfluidic flow was then switched to a perfusion of medium supplemented with 1 mmol/L diamide for 5 min. Cells responded to this oxidative challenge by rapid transition from a highly reduced steady state to a fully oxidized state within seconds. Next, the microfluidic flow was returned to diamide-free medium in which the mitochondrial sensor

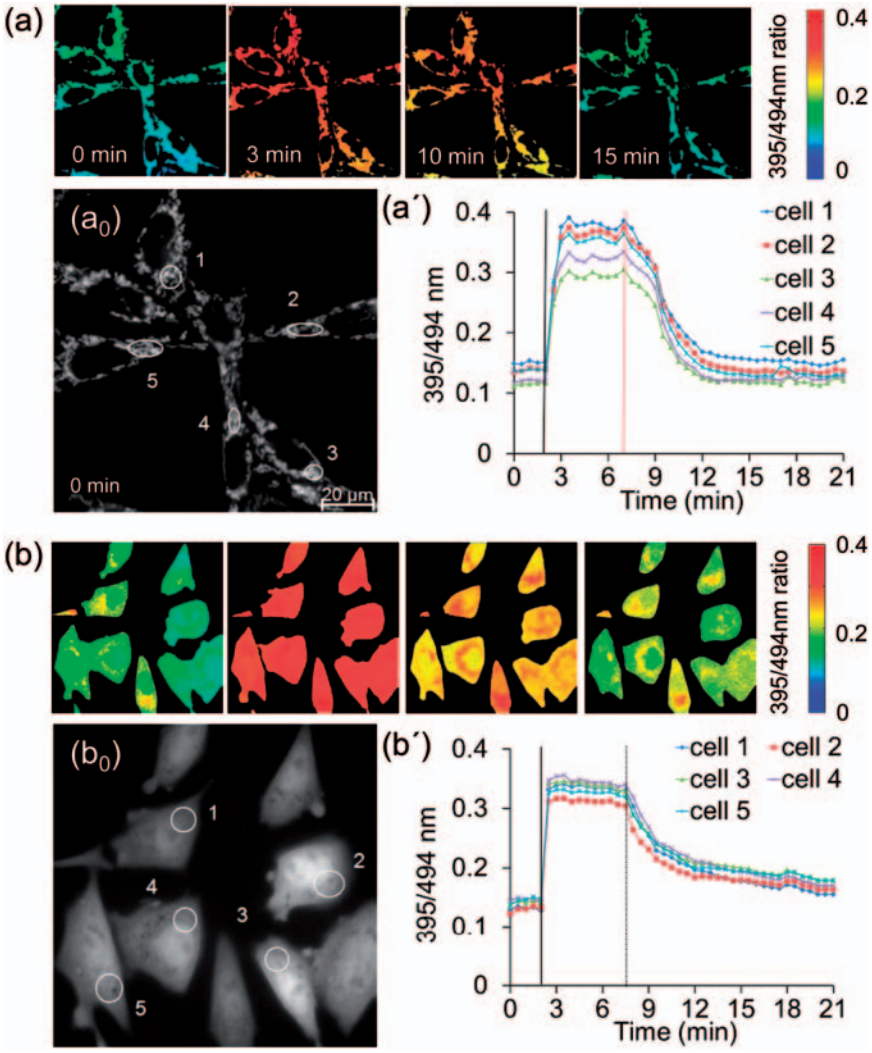

Figure 1 Acute restoration of resting glutathione redox potentials in mitochondrial matrix and cytosol after an oxidative insult. Perfusion of resting CHO cells with 1 mmol/L diamide for 5 min rapidly transitioned from a highly reduced steady state to a fully oxidized state within seconds. Microfluidic flow was then returned to diamide-free medium in which the recovery of mitochondrial (a, a′) and cytosolic (b, b′) glutathione redox poise occurred within a half time of 3 min. Fluorescence emission (494 nm) micrographs demonstrate the Grx1-roGFP2 sensor targeted to mitochondria (a_0) or cytosol (b_0) in a microfluidic channel at $t = 0$. False-color ratio images of the cells at indicated time points provide visual confirmation of mitochondrial matrix (a) and cytosol (b) recovery. Corresponding ratiometric data of ROIs are presented in panels (a′) and (b′). Vertical lines mark the initiation of diamide insult (solid line) and wash-out (dotted line)

recovered to its initial redox state with half time of 160 ± 6 s (Figure 1a′). While the initial slope of the cytosolic probe recovery was steeper, full recovery was not observed within the same time necessary for the mitochondrial probe. Nevertheless, half time of the cytosolic recovery of 155 ± 12 s was close to that of the mitochondrial matrix (Figure 1b′). Figure 1(a) and 1(b) is false-colored microscopic images that illustrate the dramatic change in the 395/494 nm excitation ratio after exposure to diamide and its wash-out at indicated time points. As depicted in the color scale bar, red corresponds to full sensor oxidation following exposure to the diamide-supplemented medium. The rapid transition towards a low 395/494 nm ratio (green/blue) indicates that diamide treatment does not cause irreversible damage under our experimental conditions. In full contrast to its behavior in plant cells, the recovery of our mitochondrial sensor was pronounced and complete after 5 min, while recovery of the cytosolic sensor was more gradual. It should be noted that compartmental recovery is dependent upon the duration of diamide exposure (Figure S2). For instance, after 2 min of oxidative challenge half time for the recovery was 77 s and 48 s for the mitochondrial matrix and cytosol, respectively. Regardless of oxidative duration with diamide (1 mmol/L), the slope of immediate recovery was similar within respective compartments (Figures 1 and S2). Thus, our data demonstrate that fully oxidized redox poise of cytosol and mitochondria is rapidly reversed upon removal of an acute oxidative insult.

Inhibition of GSH synthesis distinctly alters redox poise of mitochondrial matrix and cytosol

Although isolated mitochondria have been extensively studied, much less is known about integration of mitochondrial function within living cells. Due to the complex interplay between mitochondria and other organelles,

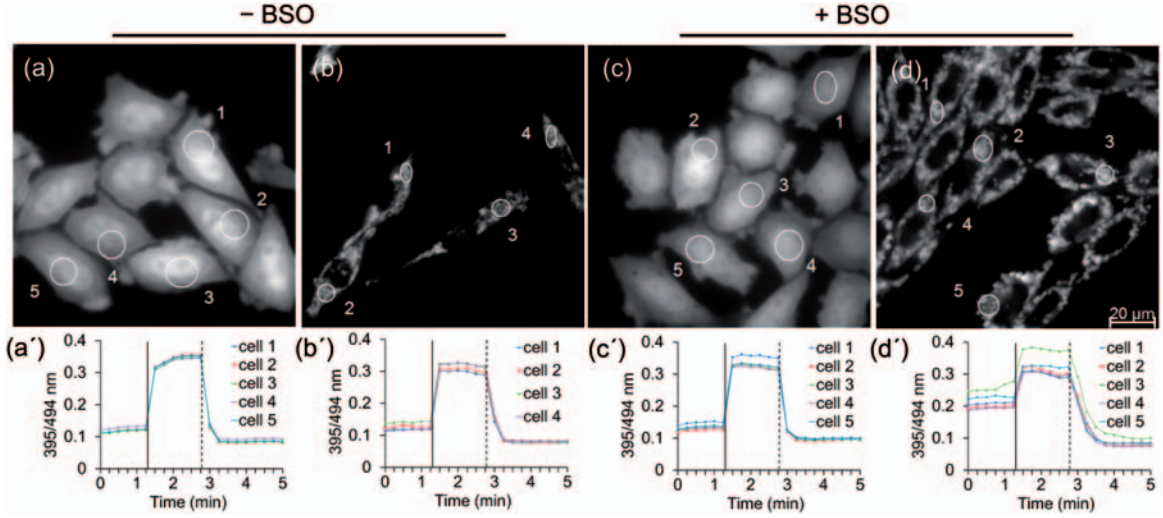

Figure 2 Differential redox response of mitochondrial matrix and cytosol to inhibition GSH synthesis. Representative images are shown of the Grx1-roGFP2 sensor targeted to cytosol (a, c) or mitochondria (b, d) in CHO cells before (a, a′, b, b′) or after (c, c′, d, d′) treatment with 0.1 mmol/L BSO for 24 h. Panels (a′-d′) are corresponding time-lapse responses of the 395/494 nm ratio to sequential treatment with diamide (vertical solid line) and DTT (vertical dashed line). Each trace within panels (a′-d′) designates a separate cell depicted on the images. The data are representative of three independent experiments with multiple wells using a minimum of four ROIs per well

Table 1 Alterations of cytosolic glutathione poise in response to inhibition of GSH synthesis

Treatment	CHO	PF161-C	PF161-T − p53^{DD}	PF161-T + p53^{DD}
−BSO	0.86 ± 0.04, $n = 40$	0.81 ± 0.03, $n = 16$	0.80 ± 0.10, $n = 20$	0.84 ± 0.08, $n = 43$
+BSO	0.80 ± 0.06, $n = 30$	0.67 ± 0.13, $n = 13$	0.67 ± 0.09, $n = 36$	0.51 ± 0.14, $n = 62$
ΔR	0.06 ± 0.07	0.14 ± 0.14	0.13 ± 0.13	0.33 ± 0.16
ΔE_{GSH}	5.6	9.9	8.7	21.7

Glutathione redox potentials were monitored with Grx1-roGFP2 targeted to cytosol of various mammalian cells. Cells were treated with or without 0.1 mmol/L BSO for 24 h. The data represent means of the fraction of the probe in the reduced form, R ± SD for three experiments; *n* – number of analyzed cells. Differences of R between the untreated and BSO-treated PF161 cells were statistically significant ($P < 0.001$, ANOVA). Significant difference was not observed between untreated and BSO-treated CHO cells ($P > 0.05$, ANOVA).
CHO: Chinese hamster ovary; PF161-C: porcine fibroblast control (non-tumorigenic) cells; PF161-T − Δp53^{DD} and PF161-T + Δp53^{DD}: isogenic tumorigenic cells; BSO: buthionine sulphoximine; ΔE_{GSH}: change in cytosolic glutathione poise between control and BSO-treated cells in mV was calculated by the Nernst equation using corresponding means of R values.

further investigation of mitochondria within viable cells is imperative. To determine the extent to which silencing of GSH synthesis affects redox poise of cytosol and mitochondrial matrix, cells were incubated with or without 0.1 mmol/L BSO, a potent inhibitor of GSH synthesis, for 24 h. Representative fluorescence microscope images of the subcellular distribution pattern of cytosolic and mitochondrial Grx1-roGFP2 with corresponding ratiometric analysis are shown in Figure 2. The background-corrected fluorescence signals of the probe acquired from individual excitation wavelength were used to calculate the 395/494 nm excitation ratio for selected ROIs (Figure 2(a) to (d)) as a function of time (Figure 2(a′) to (d′)). To determine the extent of Grx1-roGFP2 oxidation at steady state, the probe was calibrated by consecutive addition of diamide and DTT to full oxidation (100% oxidation) and reduction (0% oxidation), respectively.[19,22] Probes targeted to subcellular compartments of BSO-free CHO cells (Figure 2a′, b′) were highly reduced with a small but significant difference ($P < 0.001$) in the extent of mitochondrial and cytosolic sensor reduction of 71.5% and 85.6%, respectively (Tables 1 and 2). Therefore, consistent with previous reports,[1,30] we confirmed that at steady state the highly reduced GSH/GSSG thiol/disulfide redox couple within cytosol and mitochondrion is not at equilibrium. It should be noted that due to the inclusion of pH as a factor in the Nernst equation the E_{GSH} of mitochondrial matrix is generally considered more reduced than that of cytosol due to its higher pH, which ranges from 7.7 to 8.2, relative to a more acidic cytosolic pH which is close to 7.[15–18]

Next, we compared subcellular sensor responses between BSO-treated (Figure 2(c) and (d)) and BSO-free cells (Figure 2(a) and (b)). Figure 2c′ presents a ratiometric analysis of the cytosolic probe expressed in cells exposed to BSO treatment. Visual comparison of Figure 2a′ (BSO-free) and 2 c′ (BSO-treated) reveals the similarity of their profiles.

Table 2 Alterations of mitochondrial matrix glutathione poise in response to inhibition of GSH synthesis

Treatment	CHO	PF161-C	PF161-T − p53^{DD}	PF161-T + p53^{DD}
− BSO	0.72 ± 0.09, $n = 55$	0.55 ± 0.11, $n = 18$	0.68 ± 0.11, $n = 68$	0.69 ± 0.07, $n = 45$
+ BSO	0.33 ± 0.15, $n = 37$	0.25 ± 0.11, $n = 21$	0.29 ± 0.12, $n = 36$	0.32 ± 0.17, $n = 32$
ΔR	0.39 ± 0.18	0.30 ± 0.16	0.39 ± 0.16	0.37 ± 0.19
ΔE_{GSH}	21.6	17	21.5	20.3

Glutathione redox potentials were monitored with Grx1-roGFP2 targeted to mitochondrial matrix of various mammalian cells. Cells were treated with or without 0.1 mmol/L BSO for 24 h. The data represent means of the fraction of the probe in the reduced form, R ± SD for three experiments; *n* – number of analyzed cells. Differences of R between the untreated and BSO-treated cells were statistically significant ($P < 0.001$, ANOVA).
CHO: Chinese hamster ovary; PF161-C: porcine fibroblast control (non-tumorigenic) cells; PF161-T − Δp53^{DD} and PF161-T + Δp53^{DD}: isogenic tumorigenic cells; BSO: buthionine sulphoximine; ΔE_{GSH}: change in mitochondrial matrix glutathione poise between control and BSO-treated cells in mV was calculated by the Nernst equation using corresponding means of R values.

Table 3 BSO response in glutathione content

Treatment	CHO	PF161-C	PF161-T − p53^{DD}	PF161-T + p53^{DD}
−BSO	1575.1 ± 108	335.7 ± 59	235 ± 35	221.7 ± 38
+BSO	72.8 ± 19	147 ± 25	182.8 ± 10	176.6 ± 28
Δ %	95.4	56.2	22.2	20.3

Intracellular glutathione values determined with monochlorobimane are expressed by the geometric mean fluorescence intensity ± SD ($n = 3$). Various cell lines were treated with or without 0.1 mmol/L BSO for 24 h. Significant differences were observed between the non- and BSO-treated data ($P < 0.01$, ANOVA).
CHO: Chinese hamster ovary; PF161-C; porcine fibroblast control (non-tumorigenic) cells; PF161-T − Δp53^{DD} and PF161-T + Δp53^{DD}: isogenic tumorigenic cells; BSO: buthionine sulphoximine.

Indeed, no significant difference in the degree of oxidation of the cytosolic sensor was observed in BSO-treated cells (Table 1). While this result is consistent with previous findings, it should be noted that reaction with mBCl, a common technique for measuring GSH in cultured cells, revealed the decrease of GSH to less than 5% of control (Table 3).[43] In contrast, the mitochondrial sensor showed substantial, statistically significant ($P < 0.001$) change in oxidation in BSO-treated cells (Figure 2b′, d′ and Table 2). These results demonstrate that cytosol of CHO cells with impaired GSH synthesis resist oxidative stress, while significant oxidation of 20 mV was generated in the mitochondrial matrix with BSO treatment. Furthermore, evidence that mitochondrial oxidation via impaired GSH synthesis occurs in a broader variety of cells was demonstrated using the GL261 glioma and HEK293 embryonic kidney cell lines (Figures S3 and S4).

BSO-treated cells reveal a contributory role of p53 to cytosolic but not mitochondrial glutathione poise

The importance of the tumor suppressor p53 in the regulation of cellular metabolic processes and, specifically, cellular redox state is increasingly recognized.[33,35] To further investigate how interactions between GSH synthesis and p53 may influence compartmental glutathione redox potentials of cancer cells, the Grx1-roGFP2 sensor was targeted to mitochondrial matrix and cytosol of non-transformed, porcine fibroblast PF161-C (control) cells and isogenic tumorigenic cell lines, with (PF161-T + Δp53^{DD}) or without (PF161-T − Δp53^{DD}) impaired function of p53 (Figures 3 and 4).[44] In contrast to the cytosol, the redox potential of mitochondrial matrix is near the midpoint potential of roGFP2 making the probe ideal for studying changes of mitochondrial glutathione poise under both oxidative and reductive challenge. Figure 3 compares the extent of reduction of the mitochondrial probe in normal and cancer cells with or without alteration of GSH synthesis. In BSO-free cells, the fraction of the probe in reduced form was modestly but significantly ($P < 0.001$) larger in both cancer lines than in control cells (Table 2). These results indicate a more reduced matrix environment in tumorigenic fibroblast PF161-T relative to parental PF-161-C cells assuming metabolic alterations of the former have not caused an acidic pH shift. We next compared the redox state of the mitochondrial probe between BSO-treated and BSO-free PF161 cells. Figure 3d′-f′ illustrates high 395/494 nm excitation ratio of the probe at steady state (first minute of time lapse) in three lines of BSO-treated cells. This result indicates a similar level of oxidation of the mitochondrial matrix in all cell lines subjected to BSO. Statistical analysis of these measurements shows that the differences in change of glutathione poise observed between control and BSO-treated cells were significant ($P < 0.001$) and similar to that in CHO cells (Table 2). No significant difference in the degree of matrix oxidation was found among BSO-treated PF161-T cells. Consequently, BSO response between mitochondrial sensors of both tumor PF161-T cell lines was independent of p53 status (Figure 3). Furthermore, the mitochondrial

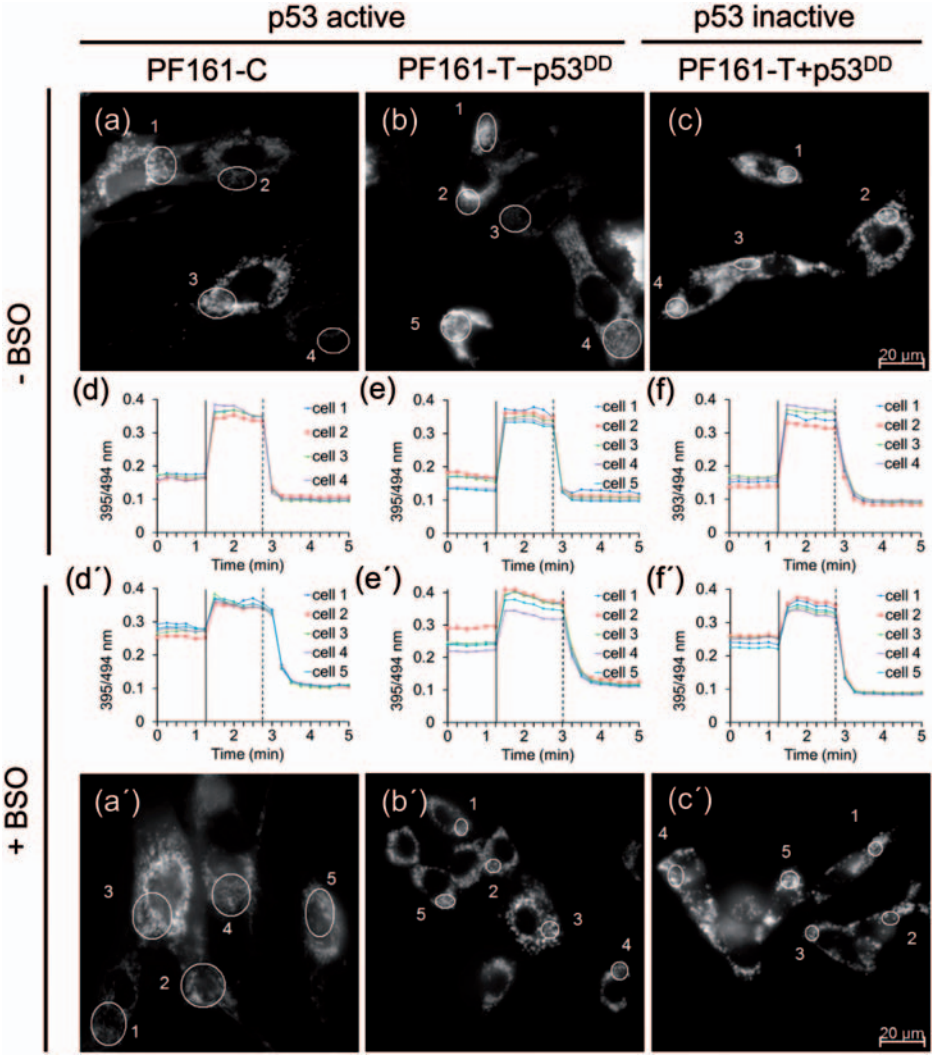

Figure 3 Glutathione poise of mitochondrial matrix is independent of p53 status of GSH-deficient tumor cells. Mito-Grx1-roGFP2 expressed in control non-transformed PF161-C (a, d, a′, d′), and isogenic PF161-T − $\Delta p53^{DD}$ (b, e, b′, e′) and PF161-T + $\Delta p53^{DD}$ (c, f, c′, f′) transformed fibroblasts without or with inactivation of the p53 pathway by expression of a dominant-negative p53 protein ($p53^{DD}$), respectively. Fluorescence emission (494 nm) micrographs showing three cell lines imaged at steady state ($t = 0$) without (a-c) or with (a′-c′) incubation 0.1 mmol/L BSO for 24 h. Corresponding time-lapse responses of Grx1-roGFP2 sensor as 395/494 nm excitation ratio to sequential treatment with diamide (vertical solid line) and DTT (vertical dashed line) are presented in panels d – f without or with (d′-f′) BSO incubation. Each trace within panels d – f and d′-f′ designates a separate cell. The data are representative of three independent experiments with multiple wells using a minimum of four ROIs per well

matrix was oxidized to approximately the same 20 mV observed in PF161-C and CHO cells, although depletion of GSH in PF161-T cells was less pronounced compared to the non-tumorigenic cells (Tables 2 and 3).

We then compared BSO responses between cytosol of distinct PF161 cell lines. At steady state BSO-free PF161 cells typically displayed no significant difference in the degree of cytosolic oxidation between lines (Table 1). However, in contrast to CHO cells, cytosol of PF161 cell lines responded to BSO treatment with increased oxidation. The change of the probe fraction in the reduced form was modest but significant in all PF161 cell lines ($P < 0.001$). Furthermore, the response to BSO was stronger in PF161-T + $\Delta p53^{DD}$ cells (21.7 mV), where the p53 pathway is inactivated by expression of a dominant-negative p53 protein (Figure 4 and Table 1).[44,45] These results demonstrate that in BSO-treated cells the fraction of the cytosolic probe in the reduced form of PF161-T + $\Delta p53^{DD}$ cells (0.51) was slightly but significantly higher ($P < 0.001$) than that of PF161-T − $\Delta p53^{DD}$ cells (0.67) (Table 1). Thus, cytosolic, but not mitochondrial, redox poise is affected by p53 status of BSO-treated PF161-T cancer cells (Figures 3 and 4).

Further comparison of BSO responses in the cytosol and matrix of the PF161 cell lines revealed nearly a two-fold change in mitochondrial glutathione potential (17 mV and 21.5 mV) relative to the cytosolic probe (9.9 mV and 8.7 mV) in BSO-treated PF161-C and PF161-T − $\Delta p53^{DD}$ cells, respectively. Conversely, both compartments responded similarly to GSH deficiency in PF161-T + $\Delta p53^{DD}$ cells (Tables 1 and 2). These experiments provide clear evidence that the GSH/GSSG thiol/disulfide redox couple within cytosol and mitochondrion is not only maintained at distinct resting redox potentials but also that cytosolic E_{GSH} is more responsive to p53 status.

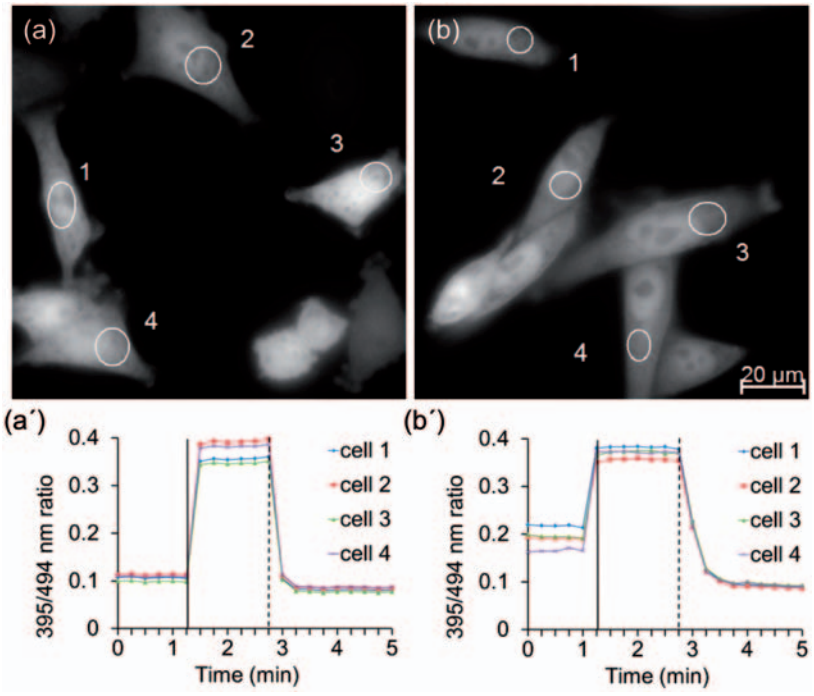

Figure 4 Cytosolic glutathione poise is affected by p53 status in GSH-deficient tumor cells. Fluorescence emission (494 nm) images of Grx1-roGFP2 probe targeted to cytosol of PF161-T + $p53^{DD}$ cells untreated (a) or treated with (b) 0.1 mmol/L BSO for 24 h. Corresponding time-lapse responses of the Grx1-roGFP2 sensor as the 395/494 nm excitation ratio to sequential treatment with diamide (solid line) and DTT (dashed line) are presented in panels a′ and b′. Each trace within panels designates a separate cell. The data are representative of three independent experiments with multiple wells using a minimum of four ROIs per well

Discussion

Under normal physiological conditions, GSH is the principal functional antioxidant to counterbalance ROS generated primarily by mitochondria. In this study, the comparison of changes in E_{GSH} between mitochondrial matrix and cytosol after inhibiting glutathione synthesis was performed using a recently developed roGFP fused to human glutaredoxin to improve specificity and rapid equilibration between the probe and subcellular glutathione redox couple.[21,26] We observed that the mitochondrial matrix is fully recovered within minutes of termination of an acute oxidative insult, indicating that the antioxidant defense capacities in this mitochondrial compartment are similar to those in the cytosol of mammalian cells. This is in stark contrast to plant cells where recovery of the mitochondrial matrix did not occur in the same time frame as in the cytosolic environment.[30]

Intracellular GSH loss is an early hallmark of the progression to cell death in response to different endogenous and exogenous stimuli. The precise contributions of cytosolic versus mitochondrial GSH pools in intracellular signaling and apoptosis, however, are not fully understood.[46] GSH synthesis can be selectively decreased by BSO, which inhibits the gamma-glutamylcysteine synthetase that catalyzes the first step in GSH synthesis.[47] The effects of BSO on mammalian cell thiol content and ROS production are described elsewhere, and the relationship between GSH deficiency and subcellular oxidation depends on the dose and duration of BSO treatment.[47,48] Recent data obtained with genetically encoded redox-sensitive probes reveal an absence of cytosolic oxidation in rat hippocampal cells after overnight incubation with BSO.[43] However, more extended treatment with BSO (72 h) significantly oxidized roGFP1 targeted to cytosolic and mitochondrion matrix compartments of human skin fibroblasts.[2] Cytosolic roGFP2 was also completely oxidized in *Arabidopsis* roots after seven-day exposure to 1 mmol/L BSO.[49]

To study if inhibition of GSH synthesis equally perturbs redox poise in cytosol and mitochondrial matrix, we altered glutathione homeostasis with BSO, a highly specific inhibitor of GSH synthesis. These data further demonstrate that changes in glutathione poise are compartmentalized, i.e. distinctly regulated, in response to inhibition of GSH biosynthesis between the cytosol and mitochondrial matrix. Stronger oxidation of the mitochondrial matrix as compared to cytosol was observed in CHO, PF161-C, and PF161-T – $\Delta p53^{DD}$ cells with active p53. A comparable BSO response was also observed in mitochondrial matrix of HEK293 embryonic kidney and GL261 glioma cells. Thus, it can be concluded that despite a similar GSH concentration in BSO-free cells, the mitochondrial matrix is characterized by an increased susceptibility to GSH deficiency than the cytosol.[12] This may indicate either an increase in the GSH turnover rate or a decrease in mitochondrial antioxidant activity in response to oxidative stimuli. We hypothesize that the similar oxidation of mitochondrial matrix of 20 mV observed in numerous cell lines despite large differences in GSH depletion may indicate a crucial threshold above which further oxidation leads to irreversible damage and consequential cell death. These differences likely reflect inherent variation in metabolic

state among the various cell lines. This is in agreement with previous studies demonstrating that inhibition of GSH synthesis causes mitochondrial damage.[7] Furthermore, recent evidence indicates that selective depletion of mitochondrial GSH sensitizes cells to oxidative stress and subsequently to stress-induced apoptosis.[15,46] Of note, calculated changes in E_{GSH} reflect pH-independent changes of glutathione couple in the pH range 5.5–8.0. However, it is not possible to completely rule out a contribution of pH to the changes in E_{GSH} especially with a comparison of various cell lines. Studies with simultaneous monitoring of glutathione poise and pH in single cells are needed to precisely determine the contribution of pH to subcellular E_{GSH}. Recent parallel analysis of live yeasts harboring roGFP2 or pHluorin, a genetically encoded pH sensor, enabled determination of pH-adjusted subcellular redox potentials in a non-invasive manner, and demonstrated that exposure to the superoxide generator paraquat, affected neither pH nor glutathione homeostasis, while hydrogen peroxide triggered alterations in both pH and the GSH/GSSG ratio.[42]

The mitochondrial matrix glutathione poise in roGFP2-harboring non-transformed PF161-C and PF161-T $-\Delta p53^{DD}$ and PF161-T $+\Delta p53^{DD}$ fibroblasts responded to inhibition of GSH synthesis by a similar 20 mV oxidation. Therefore, oxidation of mitochondrial matrix is independent of the p53 status of transformed fibroblasts. Conversely, cytosolic BSO response in cancer cells depends upon p53 status. These results indicate that activity of p53 is crucial in maintaining inherently reduced cytosolic redox poise in GSH-deficient cancer cells. On the other hand, recent data indicate that oxidative stress induced by GSH depletion enhances glutathionylation and, as a result, may decrease p53 activity.[50,51] Thus, glutathionylation of p53 may diminish its role in maintaining the reduced cytosolic environment.

Under our experimental conditions, the change in cytosolic glutathione poise in CHO or PF161-C cells is modest in spite of a large decrease in intracellular GSH pools. This moderate change of E_{GSH} indicates only minor alteration of GSH/GSSG ratio. Thus, we speculate that GSH recycling capacity effectively maintains the low levels of GSSG following GSH deficiency. Nevertheless, extended inhibition of GSH synthesis overrides antioxidant buffering capacity of the cytosol and fully oxidizes the redox-sensitive probe.[2,49]

The ability to monitor temporal changes in the redox status of various subcellular compartments of live cells in response to impaired GSH biosynthesis or other physiologically relevant stimuli will facilitate the understanding of the roles of individual compartments in vital biological processes such as proliferation, apoptosis, and cell death. Because commonly used radio- and chemotherapeutic drugs influence tumor outcome through ROS modulation, understanding the contributions of compartmentalized glutathione poise to ROS generation is also highly significant for cancer therapy.[52,53]

Author contributions: All authors participated in interpretation of the studies, analysis of the data and review of the manuscript; VLK, PJAK, and HRG participated in the experimental design, VLK, WPH, JNB, DEB, and SJD conducted the experiments, VLK, JNB, and HRG wrote the manuscript.

ACKNOWLEDGMENTS

The authors thank Dr. Barbara Pilas of the Roy J. Carver Biotechnology Center Flow Cytometry Facility and Dr. Shiv Sivaguru of the Institute for Genomic Biology for their assistance. This work was supported by National Institutes of Health Grant: R33-CA137719 (PJA Kenis and HR Gaskins).

REFERENCES

1. Schafer FQ, Buettner GR. Redox environment of the cell as viewed through the redox state of the glutathione disulfide/glutathione couple. *Free Radic Biol Med* 2001;**30**:1191–212
2. Jones DP. Redefining oxidative stress. *Antioxid Redox Signal* 2006;**8**:1865–79
3. Verkaart S, Koopman WJ, Cheek J, van Emst-de Vries SE, van den Heuvel LW, Smeitink JA, Willems PH. Mitochondrial and cytosolic thiol redox state are not detectably altered in isolated human NADH:ubiquinone oxidoreductase deficiency. *Biochimica et Biophysica Acta* 2007;**1772**:1041–51
4. Morgan B, Sobotta MC, Dick TP. Measuring E(GSH) and H2O2 with roGFP2-based redox probes. *Free Radic Biol Med* 2011;**51**:1943–51
5. Naviaux RK. Oxidative shielding or oxidative stress? *J Pharmacol Exp Ther* 2012;**342**:608–18
6. Valko M, Rhodes CJ, Moncol J, Izakovic M, Mazur M. Free radicals, metals and antioxidants in oxidative stress-induced cancer. *Chem Biol Interact* 2006;**160**:1–40
7. Meister A. Glutathione deficiency produced by inhibition of its synthesis, and its reversal; applications in research and therapy. *Pharmacol Ther* 1991;**51**:155–94
8. Dickinson DA, Forman HJ. Glutathione in defense and signaling: lessons from a small thiol. *Ann N Y Acad Sci* 2002;**973**:488–504
9. Hansen JM, Go YM, Jones DP. Nuclear and mitochondrial compartmentation of oxidative stress and redox signaling. *Annu Rev Pharmacol Toxicol* 2006;**46**:215–34
10. Jones DP. Disruption of mitochondrial redox circuitry in oxidative stress. *Chem Biol Interact* 2006;**163**:38–53
11. Kemp M, Go Y-M, Jones DP. Nonequilibrium thermodynamics of thiol/disulfide redox systems: a perspective on redox systems biology. *Free Radic Biol Med* 2008;**44**:921–37
12. Mari M, Morales A, Colell A, Garcia-Ruiz C, Fernandez-Checa JC. Mitochondrial glutathione, a key survival antioxidant. *Antioxid Redox Signal* 2009;**11**:2685–700
13. Go YM, Jones DP. Redox compartmentalization in eukaryotic cells. *Biochim Biophys Acta* 2008;**1780**:1273–90
14. Ayer A, Fellermeier S, Fife C, Li SS, Smits G, Meyer AJ, Dawes IW, Perrone GG. A genome-wide screen in yeast identifies specific oxidative stress genes required for the maintenance of sub-cellular redox homeostasis. *PLoS One* 2012;**7**:e44278
15. Muyderman H, Wadey AL, Nilsson M, Sims NR. Mitochondrial glutathione protects against cell death induced by oxidative and nitrative stress in astrocytes. *J Neurochem* 2007;**102**:1369–82
16. Merksamer PI, Trusina A, Papa FR. Real-time redox measurements during endoplasmic reticulum stress reveal interlinked protein folding functions. *Cell* 2008;**135**:933–47
17. Waypa GB, Marks JD, Guzy R, Mungai PT, Schriewer J, Dokic D, Schumacker PT. Hypoxia triggers subcellular compartmental redox signaling in vascular smooth muscle cells. *Circ Res* 2010;**106**:526–35
18. Kojer K, Bien M, Gangel H, Morgan B, Dick TP, Riemer J. Glutathione redox potential in the mitochondrial intermembrane space is linked to the cytosol and impacts the Mia40 redox state. *Embo J* 2012;**31**:3169–82

19. Dooley CT, Dore TM, Hanson GT, Jackson WC, Remington SJ, Tsien RY. Imaging dynamic redox changes in mammalian cells with green fluorescent protein indicators. *J Biol Chem* 2004;**279**:22284–93
20. Lohman JR, Remington SJ. Development of a family of redox-sensitive green fluorescent protein indicators for use in relatively oxidizing subcellular environments. *Biochemistry* 2008;**47**:8678–88
21. Gutscher M, Pauleau AL, Marty L, Brach T, Wabnitz GH, Samstag Y, Meyer AJ, Dick TP. Real-time imaging of the intracellular glutathione redox potential. *Nat Met* 2008;**5**:553–9
22. Hanson GT, Aggeler R, Oglesbee D, Cannon M, Capaldi RA, Tsien RY, Remington SJ. Investigating mitochondrial redox potential with redox-sensitive green fluorescent protein indicators. *J Biol Chem* 2004;**279**:13044–53
23. Hu J, Dong L, Outten CE. The redox environment in the mitochondrial intermembrane space is maintained separately from the cytosol and matrix. *J Biol Chem* 2008;**283**:29126–34
24. Schwarzlander M, Fricker MD, Muller C, Marty L, Brach T, Novak J, Sweetlove LJ, Hell R, Meyer AJ. Confocal imaging of glutathione redox potential in living plant cells. *J Microsc* 2008;**231**:299–316
25. Ayer A, Tan SX, Grant CM, Meyer AJ, Dawes IW, Perrone GG. The critical role of glutathione in maintenance of the mitochondrial genome. *Free Radic Biol Med* 2010;**49**:1956–68
26. Meyer AJ, Dick TP. Fluorescent protein-based redox probes. *Antioxid Redox Signal* 2010;**13**:621–50
27. Sena LA, Chandel NS. Physiological roles of mitochondrial reactive oxygen species. *Mol Cell* 2012;**48**:158–67
28. Murphy MP. Mitochondrial thiols in antioxidant protection and redox signaling: distinct roles for glutathionylation and other thiol modifications. *Antioxid Redox Signal* 2012;**16**:476–95
29. Mari M, Morales A, Colell A, Garcia-Ruiz C, Kaplowitz N, Fernandez-Checa JC. Mitochondrial glutathione: features, regulation and role in disease. *Biochim Biophys Acta* 2013;**1830**:3317–28
30. Schwarzlander M, Fricker MD, Sweetlove LJ. Monitoring the in vivo redox state of plant mitochondria: effect of respiratory inhibitors, abiotic stress and assessment of recovery from oxidative challenge. *Biochim Biophys Acta* 2009;**1787**:468–75
31. Enns L, Ladiges W. Mitochondrial redox signaling and cancer invasiveness. *J Bioenerg Biomembr* 2012;**44**:635–8
32. Cui X. Reactive oxygen species: the achilles' heel of cancer cells? *Antioxid Redox Signal* 2012;**16**:1212–4
33. Liu B, Chen Y, St Clair DK. ROS and p53: a versatile partnership. *Free Radic Biol Med* 2008;**44**:1529–35
34. Pani G, Galeotti T. Role of MnSOD and p66shc in mitochondrial response to p53. *Antioxid Redox Signal* 2011;**15**:1715–27
35. Maillet A, Pervaiz S. Redox regulation of p53, redox effectors regulated by p53: a subtle balance. *Antioxid Redox Signal* 2012;**16**:1285–94
36. Puzio-Kuter AM. The role of p53 in metabolic regulation. *Genes Cancer* 2011;**2**:385–91
37. Soussi T, Beroud C. Assessing TP53 status in human tumours to evaluate clinical outcome. *Nat Rev Cancer* 2001;**1**:233–40
38. Kolossov VL, Beaudoin JN, Hanafin WP, DiLiberto SJ, Kenis PJ, Rex Gaskins H. Transient light-induced intracellular oxidation revealed by redox biosensor. *Biochem Biophys Res Commun* 2013;**439**:517–21
39. Kolossov VL, Spring BQ, Sokolowski A, Conour JE, Clegg RM, Kenis PJA, Gaskins HR. Engineering redox-sensitive linkers for genetically encoded FRET-based biosensors. *Exp Biol Med* 2008;**233**:238–48
40. Otsu N. The threshold selection method from gray-level histograms. *IEEE Trans Syst Man Cybern* 1979;**SMC-9**:62–6
41. Lin C, Kolossov VL, Tsvid G, Trump L, Henry JJ, Henderson JL, Rund LA, Kenis PJA, Schook LB, Gaskins HR, Timp G. Imaging in real-time with FRET the redox responses of tumorigenic cells to glutathione petrubations in a microscale flow. *Integr Biol* 2011;**3**:208–17
42. Ayer A, Sanwald J, Pillay BA, Meyer AJ, Perrone GG, Dawes IW. Distinct redox regulation in sub-cellular compartments in response to various stress conditions in Saccharomyces cerevisiae. *PLoS One* 2013;**8**:e65240
43. Funke F, Gerich FJ, Muller M. Dynamic, semi-quantitative imaging of intracellular ROS levels and redox status in rat hippocampal neurons. *Neuroimage* 2011;**54**:2590–602
44. Adam SJ, Rund LA, Kuzmuk KN, Zachary JF, Schook LB, Counter CM. Genetic induction of tumorigenesis in Swine. *Oncogene* 2007;**26**:1038–45
45. Willis A, Jung EJ, Wakefield T, Chen X. Mutant p53 exerts a dominant negative effect by preventing wild-type p53 from binding to the promoter of its target genes. *Oncogene* 2004;**23**:2330–8
46. Franco R, Cidlowski JA. Apoptosis and glutathione: beyond an antioxidant. *Cell Death Differ* 2009;**16**:1303–14
47. Bertsche U, Schorn H. Glutathione depletion by DL-Buthionine-SR-Sulfoximine (BSO) potentiates x-ray induced chromosome lesions after liquid holding recovery. *Radiat Res* 1986;**105**:351–69
48. Armstrong JS, Steinauer KK, Hornung B, Irish JM, Lecane P, Birrell GW, Peehl DM, Knox SJ. Role of glutathione depletion and reactive oxygen species generation in apoptotic signaling in a human B lymphoma cell line. *Cell Death Differ* 2002;**9**:252–63
49. Meyer AJ, Brach T, Marty L, Kreye S, Rouhier N, Jacquot JP, Hell R. Redox-sensitive GFP in Arabidopsis thaliana is a quantitative biosensor for the redox potential of the cellular glutathione redox buffer. *Plant J* 2007;**52**:973–86
50. Velu CS, Niture SK, Doneanu CE, Pattabiraman N, Srivenugopal KS. Human p53 is inhibited by glutathionylation of cysteines present in the proximal DNA-binding domain during oxidative stress. *Biochemistry* 2007;**46**:7765–80
51. Yusuf MA, Chuang T, Bhat GJ, Srivenugopal KS. Cys-141 glutathionylation of human p53: studies using specific polyclonal antibodies in cancer samples and cell lines. *Free Radic Biol Med* 2010;**49**:908–17
52. Sosa V, Moline T, Somoza R, Paciucci R, Kondoh H, ME LL. Oxidative stress and cancer: an overview. *Ageing Res Rev* 2013;**12**:376–90
53. Watson J. Oxidants, antioxidants and the current incurability of metastatic cancers. *Open Biol* 2013;**3**:120144

(Received July 22, 2013, Accepted December 9, 2013)